PHYSICAL REVIEW B VOLUME 59, NUMBER 4 15 JANUARY 1999-II

Steps on CdSe $(11\bar{2}0)$ and $(10\bar{1}0)$ cleavage surfaces: Evidence for crack propagation in competing cleavage planes

B. Siemens, C. Domke, Ph. Ebert,* and K. Urban
Institut für Festkörperforschung, Forschungszentrum Jülich GmbH, 52425 Jülich, Germany

(Received 29 September 1997)

We determined the structure and electronic properties of cleavage steps on CdSe $(11\bar{2}0)$ and $(10\bar{1}0)$ surfaces from atomically resolved scanning tunneling microscopy images. Steps occur in high concentrations and are always oriented parallel to the [0001] direction on both cleavage surfaces. The steps are electrically uncharged. Kinks are extremely rare and electrically charged. The edges of steps on $(11\bar{2}0)$ surfaces consist of $\{10\bar{1}0\}$ facets and steps on $(10\bar{1}0)$ surfaces exhibit $\{11\bar{2}0\}$ facets. Steps occur preferentially in pairs (one up and one down) on both surfaces. The step structure is explained by a crack propagation in neighboring cleavage planes favored by the creation of uncharged steps. [S0163-1829(99)01504-0]

I. INTRODUCTION

The structure of cleaved-crystal surfaces depends critically on the details of crack propagation and on the crystal structure. Some materials have planes that are particularly favorable for cleavage. For example, Si cleaves excellently on the (111) planes, because these planes are the most closely packed ones.[1] For polar-compound semiconductors in the zinc-blende structure the constraints of electrical neutrality of the surface created by cleavage dominate the cleavage properties. Only perfectly flat *nonpolar* (110) cleavage surfaces can be obtained, but no cleavage is possible along *polar* planes, such as the (111) plane. Cleavage can also lead to rough surfaces as in the case of Al-Pd-Mn quasicrystals, where the crack propagates between mechanically highly stable clusters. Thus, the cleavage surface exhibits the cluster-based substructure of the quasicrystal.[2] In general, the structure of the cleavage surfaces reflects the bonding strength and the structure of the material rather than the equilibrium surface properties. Thus, the investigation of the structure of cleaved surfaces on the atomic scale provides the opportunity to deduce information about the crack propagation and bonding properties in a crystal.

In this paper we investigate steps on $(10\bar{1}0)$ and $(11\bar{2}0)$ cleavage surfaces of CdSe grown in the wurtzite structure. We determine the atomic structure of the steps and show that step edges on (1120) surfaces consist of {1010} facets and step edges on (1010) surfaces exhibit {1120} facets. Kinks at steps are extremely rare and electrically charged. Kink-free steps are uncharged. It is shown that steps occur in pairs, one step upward and the next one downward. This surface morphology is explained by a mode of crack propagation in which neighboring cleavage planes are employed simultaneously. Furthermore, the electrical neutrality demonstrates that unlike the case of cubic compound semiconductors, steps do not change the electrical properties of the surface. It is suggested that the charge neutrality of the steps favors the crack propagation in competing cleavage planes present in the wurtzite structure.

II. EXPERIMENT

We investigated an *n*-type CdSe single crystal grown by the Markov growth technique. The crystal exhibited a carrier concentration of about $7\times10^{18}\,\mathrm{cm}^{-3}$. Samples with dimensions of $3\times3\times7\,\mathrm{mm}^3$ were cut from the crystal. The long axis of the samples was parallel to either the [1120] or [1010] direction. On opposite sides of each sample two cleavage slots were cut, such that the cleavage proceeds along the [0001] direction. The samples were cleaved in *ultrahigh vacuum* $(5\times10^{-9}\,\mathrm{Pa})$ along (1120) and (1010) planes using a double-wedge technique. After cleavage the crystals were immediately investigated by scanning tunneling microscopy without breaking the vacuum. Ohmic contacts were obtained by sputtering gold on two opposite faces of the samples followed by an electrical discharge of a capacitor over these contacts. We used electrochemically etched tungsten tips.

III. RESULTS

Figure 1 shows the typical surface structures observed on the $(11\bar{2}0)$ and $(10\bar{1}0)$ surfaces of CdSe. Both cleavage surfaces consist of flat terraces separated by steps. CdSe

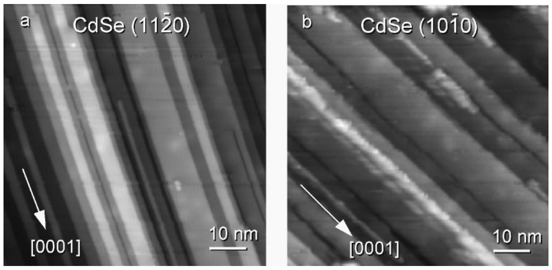

FIG. 1. Constant-current scanning tunneling microscope images of the two cleavage surfaces of CdSe. Frame (a) shows the occupied states of the $(11\bar{2}0)$ surface (measured -3.4 V sample voltage and 0.3 nA) and frame (b) the occupied states of the $(10\bar{1}0)$ surface acquired at -2.4 V and 0.2 nA. On both surfaces the steps have very few kinks and are always parallel to the [0001] direction.

0163-1829/99/59(4)/3000(8)/$15.00

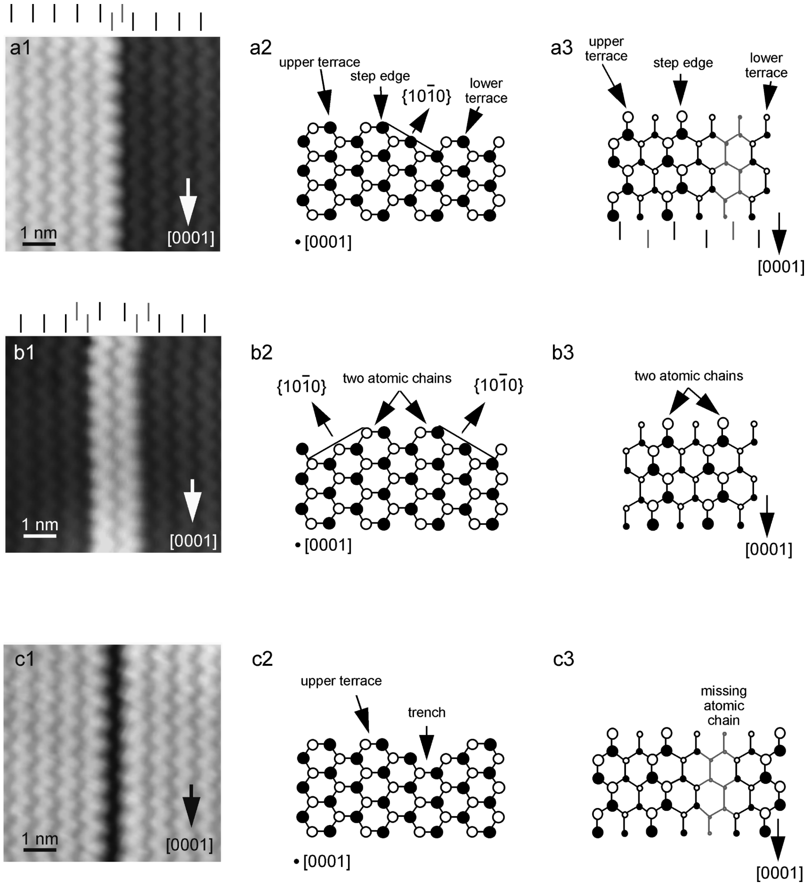

FIG. 2. High-resolution STM images of steps one atomic-layer high occurring in different configurations on the $(11\bar{2}0)$ surface of CdSe [frames labeled (a1), (b1), and (c1)]. For each image the side view [(a2), (b2), and (c2)] and top view [(a3), (b3), and (c3)] of the atomic-structure model is given. The images were measured at $+3.0$, -3.7, and -3.0 V, respectively. The tunnel current was fixed at 0.3 nA. Solid and empty circles show Se and Cd atoms, respectively.

cleavage surfaces exhibit a significantly higher density of steps compared to cleavage surfaces of cubic compound semiconductors, such as GaAs(110) surfaces obtained by the same cleavage technique. The images show that all steps are parallel to each other and oriented along the [0001] direction. No other orientations of steps were found. The terraces can be as narrow as one atomic row, but still several tenths of a nanometer long or even longer. The wider terraces reach widths of 10–15 nm. Thus, the surface is rough and not atomically smooth. Indeed, even the macroscopic cleavage surface is not as flat as, for example, GaAs(110) surfaces. We frequently observed that the cleavage did not proceed only in the desired plane, although all cleaved samples exhibited large areas of the desired surface orientation. In the following we will analyze the properties of the steps in detail.

A. Atomic structure of steps

1. Steps on the $(11\bar{2}0)$ *surfaces*

On the $(11\bar{2}0)$ surfaces we found that steps were (0.22 ± 0.02) nm high. This corresponds to a height of one atomic layer. We observed only one type of step-edge structure even if the steps occur in different configurations, such as an isolated step between two larger terraces, a terrace only one or two atomic rows wide (delimited by a pair of up-and-down steps), or a missing row inducing a pair of down-and-up steps. Figure 2 shows high-resolution images of these three configurations of steps and the respective schematic models.

At this stage we have to recall the electronic and geometric structure of the CdSe$(11\bar{2}0)$ surface. The surface has a 1×1 reconstruction[3–9] and one occupied and one empty dangling bond is localized above each Se anion and Cd cation, respectively.[10–17] These two dangling-bond states correspond to the occupied- and empty-surface states. The surface states are resonant with the valence and conduction bands at the center of the surface Brillouin zone, respectively, where the electrons are extracted or injected by the tip of the scanning tunnel microscope (STM).[18] Thus, the STM images measured at negative and positive sample voltages show the dangling bonds localized above the anions and cations, respectively.[18] With this knowledge the high-resolution STM images of the occupied states in Figs. 2(b) and 2(c) show the positions of the Se atoms, while the high-resolution image in Fig. 2(a) shows the positions of the Cd atoms. In the following this will be the basis for our analysis of the atomic structure of the steps.

First we analyze the relative location and alignment of the density of state maxima on the upper and lower terraces. For all steps the periodicity in the [0001] direction along zigzag chains is in phase on the upper and lower terraces. However, the periodic alignment of the chains measured perpendicular to the step direction is not in phase on the upper and lower terraces [see dashes above frames (a1) and (b1) of Fig. 2]. The chains are in antiphase along the direction perpendicular to the chains. The zigzag chain directly at the step edge on the upper terrace always appears wider than chains within the terraces (see Fig. 2). A quantitative analysis of the apparent width (Fig. 3) shows an increase of the width of about 50%. The increased width is only discernible for the chain directly at the step edge. Even the second chain is not affected and the average width of the chains on the lower ter-

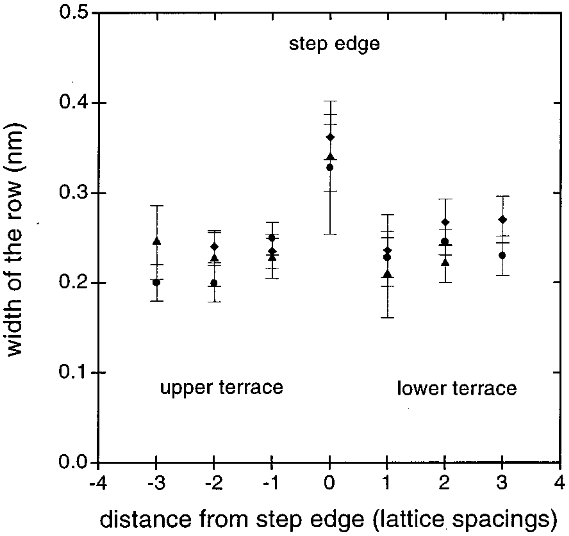

FIG. 3. Width of the atomic chain measured perpendicular to the [0001] direction across steps one atomic-layer high. The chain at the step edge is at distance 0 (chain number 0). Negative and positive values of the chain numbers (measured in lattice spacings) indicate chains on the upper and lower terrace, respectively. Only the chain at the step edge appears wider.

race is the same as on the upper terrace. The step has a ×1 periodicity along its edge. Thus, no superstructure developed. Simultaneously measured images of the occupied and empty states show that the zigzag chains of the empty and occupied states are not shifted perpendicular to the [0001] direction. High-resolution images of the empty states exhibit essentially the same characteristics as the images of the occupied states [compare, e.g., frames (a1) and (b1) in Fig. 2].

In the discussion of the atomic structure of the step edge all the above-mentioned characteristics need to be addressed adequately by a geometric model. Figure 2 shows schematic drawings of the atomic structures of the steps. The frames labeled number 2 and 3 show the side and top views, respectively. The solid circles indicate positions of Se atoms. Open circles represent Cd atoms. The model is based on a 1×1 surface unit cell, because low-energy electron diffraction and low-energy positron diffraction experiments demonstrated the existence of the 1×1 surface reconstruction.[3–8] The ×1 periodicity along the step edge rules out any superstructure due to a reconstruction of the step edge. We recall that images of the occupied and empty dangling-bond states show the positions of the Se and Cd atoms, respectively. The Se and Cd atoms form chains along the [0001] direction. If we only concentrate on the Se atoms (solid circles) the chains appear as zigzag rows. This is the structure visible in the STM images. The periodicity of the chains along the [0001] direction is in phase on the upper and lower terraces. Perpendicular to the [0001] direction the chains are out of phase on both terraces (see dashes below frame *a*3 of Fig. 2). If we focus only on the Cd atoms we observe the same features again. This is in agreement with our measurements. The larger width of the chain at the step edge is also understandable within the structural model. Below each Se atom at the step edge is another one. It has a separation of half a lattice spacing (i.e., half the separation between two zigzag chains). Both Se atoms have the same bonding configuration and, thus, occupied dangling bonds with the same spatial orientation (see Fig. 4). Since the two dangling bonds are very close to each other, they partially overlap and cannot be resolved separately by the STM. This leads to an apparently elongated dangling bond at the step edge. The same arguments apply for the empty dangling bonds of the Cd atoms at the step edge. This explanation is corroborated by the fact that the chain at the step edge is asymmetric. It appears wider only on the side toward the lower terrace. A stress field cannot explain the observed features, because it would have a larger extension and is not atomically localized at the step edge.[19] Thus, the wider chain at the step edge is the signature of the dangling bond structure and of the type of facet formed by the step edge. The surface area with different orientation at the step edge can be called a facet, because its orientation can be determined unambigiously and the step edge forms a new surface orientation at least one unit cell wide. From this we conclude that steps on the $(11\bar{2}0)$ surfaces have facets with a $\{10\bar{1}0\}$ orientation and a 1×1 reconstruction. Other facets would not agree with the high-resolution images.

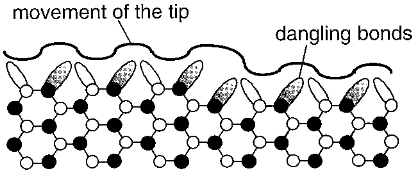

FIG. 4. Side view of a dangling bond model of a step one atomic-layer high on the CdSe $(11\bar{2}0)$ surface. The two dangling bonds at the step edge overlap leading to one apparently elongated dangling bond in the STM images (see solid line). The step edge is a facet with $\{10\bar{1}0\}$ orientation.

2. Steps on the $(10\bar{1}0)$ *surfaces*

On $(10\bar{1}0)$ surfaces we observed steps with a height of (3.8 ± 0.4) nm. This height corresponds to steps two atomic layers high. The steps occur in a variety of different configurations, such as narrow terraces and isolated missing rows produced by pairs of close steps. Figure 5 shows a high-resolution image of the occupied states of an isolated step. The rows running perpendicular to the step are in phase on the upper and lower terrace, while the rows parallel to the step in the [0001] direction are out of phase (i.e., in antiphase relation) across the step. A zigzag structure is clearly discernable at the step edge. The step edge has a ×1 periodicity. The clarity of the zigzag structure at the step edge is somewhat tip dependent, but always present. We believe that this

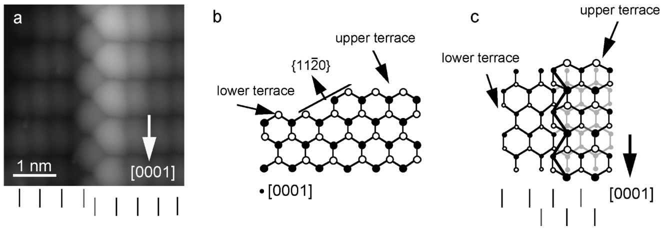

FIG. 5. (a) High-resolution STM image of a step on the CdSe $(10\bar{1}0)$ surface (measured at -2 V and 0.2 nA). (b) and (c) show a side and top view of the step model.

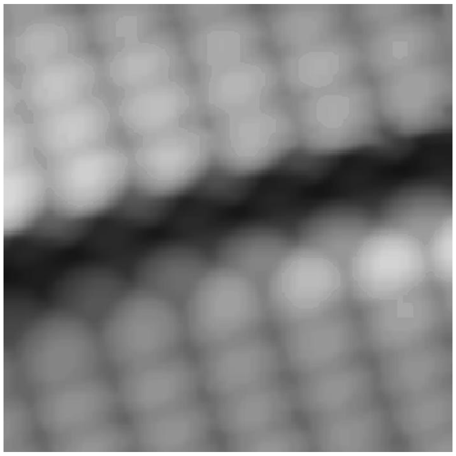

FIG. 6. High-resolution STM image of a trench delimited by two steps forming {11$\bar{2}$0}-oriented facets on the CdSe (10$\bar{1}$0) surface (measured at −2.3 V and 0.2 nA).

is due to the frequently changing resolution of the tip. In fact, tunneling on these surfaces is rather difficult due to the instability of the surface and the frequent changes of the tip state.

Frames *b* and *c* in Fig. 5 show a structural model of the isolated step on the (1010) surfaces. The model is again based on a 1×1 reconstruction. The size of the unit cell on the terraces supports this approach.[18] The ×1 periodicity along the step edge excludes any superstructure. We concentrate first on the filled circles representing the Se atoms in the model [Fig. 5(c)]. The atomic rows formed by the Se atoms (solid circles) perpendicular to the step-edge direction are in phase across the step on both terraces. However, the rows parallel to the step are out of phase (see dashes). Both results agree with the STM images. The most prominent feature is the presence of a zigzag row at the step edge. This feature is the signature of a facet with {1120} orientation and a 1×1 reconstruction. In the model the solid zigzag line indicates the Se atoms (filled circles) on the facet each having a fully occupied dangling bond. These dangling bonds on the facet give rise to the zigzag structure. In fact the zigzag structure of the facet is the same as that visible on the (1120) surface (see Fig. 2). Thus, steps on (1010) surfaces have (1120)-oriented facets. This can be particularly well seen in Fig. 6. Figure 6 shows a narrow trench. On both sides the zigzag structure indicates the presence of {1120}-oriented facets.

We only observed steps that were two atomic layers high. This indicates that the cleavage along (10$\bar{1}$0) planes is not possible to the same extent in all layers. The layers have alternatingly two and four bonds per unit cell. Thus, only the layers with two bonds per unit cell are expected to cleave well. A cleavage in the intermediate layer with four bonds to be broken leads to a high density of dangling bonds. This is expected to increase the surface energy substantially, and thus, only steps with a height of an even number of layers will occur.

B. Electronic structure of steps

1. Kink-free steps

Steps are defects, and thus can give rise to localized states in the band gap. This may lead to electrical charges associated with the steps. Indeed, on cubic III-V compound semiconductors the steps were found to be charged at kinks as well as along kink-free parts of the step.[20] However, on CdSe cleavage surfaces the situation is different. Figures 7 and 8

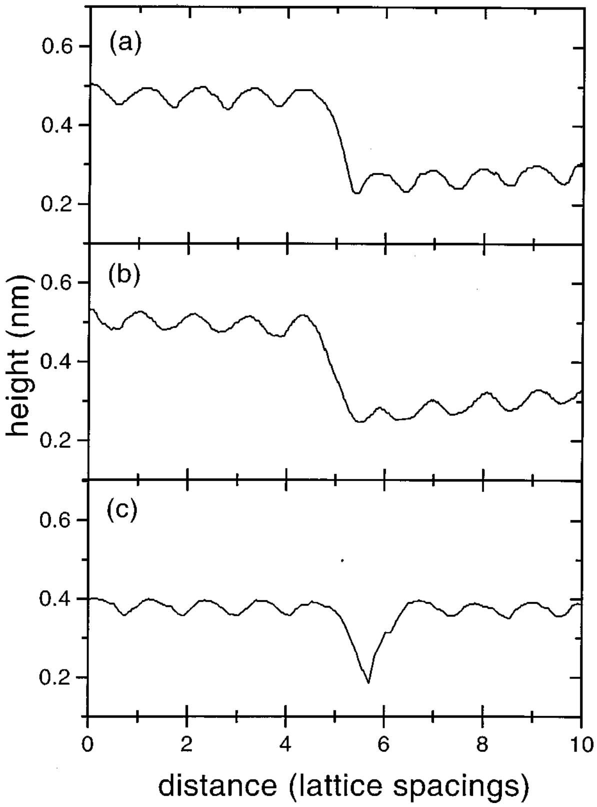

FIG. 7. Line profiles across different steps on the CdSe (11$\bar{2}$0) surface. None of the profiles exhibit a band bending as seen along steps on GaAs, InP, and GaP (110) surfaces (Ref. 20). The steps are thus uncharged.

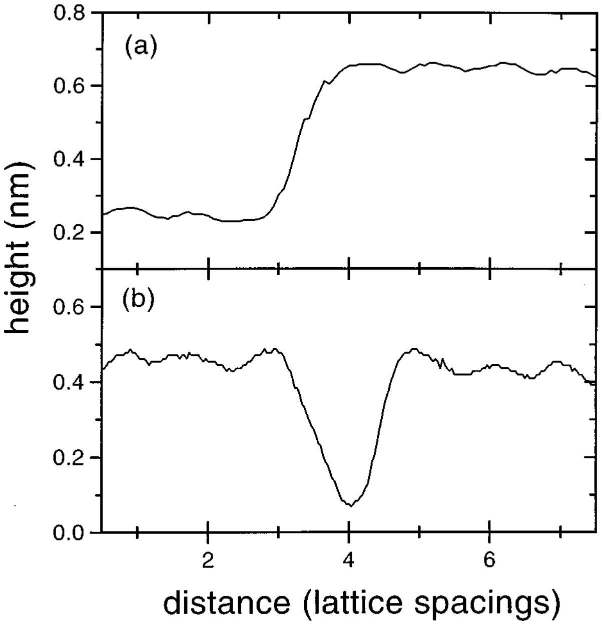

FIG. 8. Same as Fig. 7, but for steps on the CdSe (10$\bar{1}$0) surface.

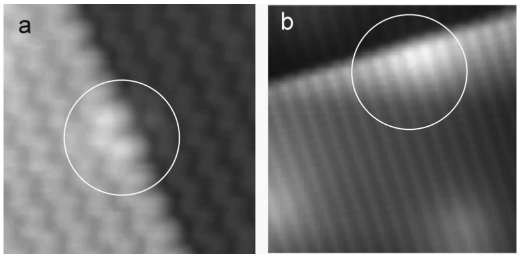

FIG. 9. STM images of a step on the (a) $(11\overline{2}0)$ and (b) $(10\overline{1}0)$ surface. There is a dopant atom at both step edges. Frames (a) and (b) were obtained at −3.7 V and 0.3 nA and −2.5 V and 0.2 nA, respectively.

show the tip height taken along a line across different steps (with no kinks) on the $(11\overline{2}0)$ and $(10\overline{1}0)$ surface, respectively. None of the profiles exhibit any long-range height change. This indicates that the steps are not surrounded by a local band bending. From this we conclude that the steps are electrically uncharged on both surfaces.

The uncharged state of the steps is further corroborated by the fact that it is possible to observe electrically active dopant atoms directly at step edges (Fig. 9). The white contrast is the signature of a dopant atom on *n*-doped surfaces.[21,22] If the steps were charged, their band bending would cover any band bending induced by a dopant atom or modify the charge state of the dopant atom. Since this is not the case, the steps cannot be charged.

2. Kinks

Figure 10(a) shows some of the rarely occurring kinks at steps on the $(11\overline{2}0)$ surface. The kinks appear brighter and the line profile in Fig. 10(b) reveals a significant height change at the kink site. This indicates a local band bending. From this we conclude that kinks carry an electrical charge. Under usual conditions the Fermi-level effect leads to a negative charge, since the dopant atoms are donors. Unfortunately, we cannot tell the polarity of the charge from the height change in the STM image, because the band bending around negative and positive charges on *n*-doped surfaces leads in both cases to an increased tunnel current from the sample to the tip.[22] Thus, the image of the occupied states appears bright for both polarities. The polarity of the charge is only deducible from the contrast of empty state images,[23] which unfortunately could not be obtained without altering the surface structure. Nevertheless, the height change indicates the presence of an electrical charge at the kink site.

C. Step-step correlations

In this section we focus on the distribution of steps. In particular, we determine whether up and down steps are randomly distributed. For this purpose we deduced from the STM images the probability of finding a downward step following an upward or a downward step as a function of the number of steps in between those two steps (Fig. 11). The values determined in Fig. 11 correspond to an one-dimensional autocorrelation function of the steps only. The error of the values is about ±5%. Figure 11 shows that there is only a correlation between directly neighboring steps (step number 1). Steps further apart do not exhibit any significant change of the probability within the error margins. For neighboring steps there is, however, a strong correlation that an upward step is followed by a downward step and vice versa. This correlation holds for both surface orientations. We note that the correlation data in Fig. 11(b) is shifted about 10% downward, because of a general small miscleavage angle. With this in mind it is obvious that both cleavage planes exhibit the same step-step correlation. Thus, on the surface pairs of upward and downward steps occur preferentially and the steps are not merely due to a general miscleavage angle of the surface. Figures 1 and 2 show some examples of typical pairs of steps, giving rise to the correlation. The data also indicates that pairs of steps are statistically independent of each other.

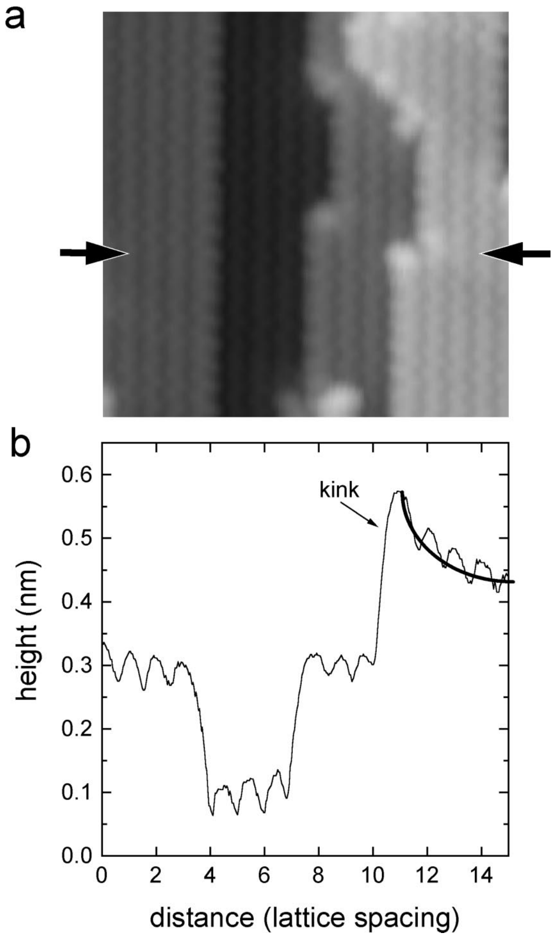

FIG. 10. STM image of kinks (a) and height change induced by a kink (b). The constant current STM image was measured at −3.7 V and 0.3 nA.

D. Tip-induced modification of steps

During scanning we sometimes observed that the tip influenced the surface morphology. The tip was able to pick up material from the surface. The removal of the material occurred mostly at kink sites. We never observed a removal of material at kink-free steps. This preferential transfer of kink atoms to the tip leads to the removal of a chain of atoms along the [0001] direction. This can be seen in the series of images shown in Fig. 12. The effects observed here have their analogy on the (110) cleavage surfaces of cubic III-V

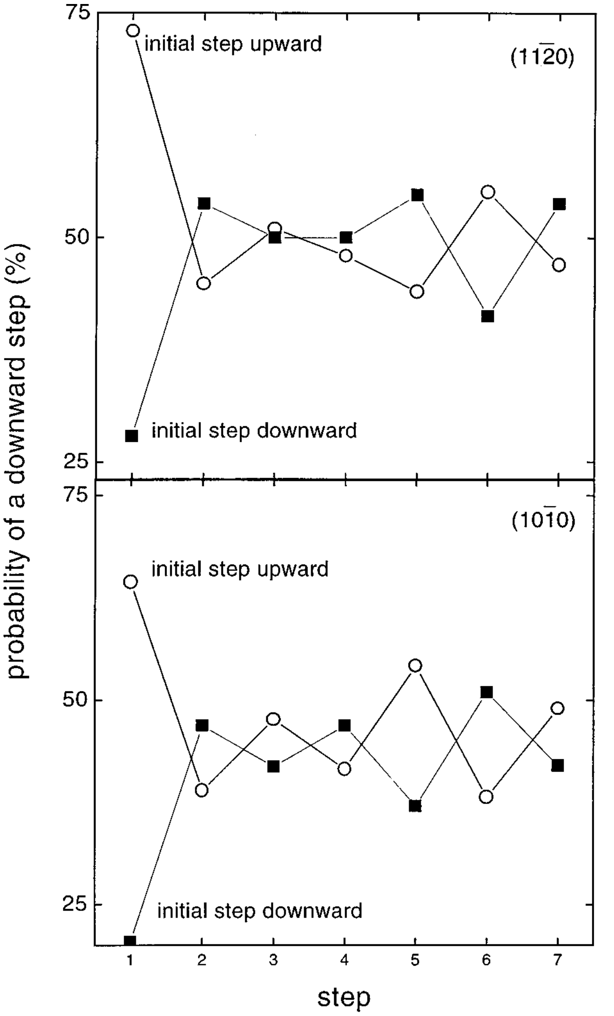

FIG. 11. Probability of finding a downward step following an upward or a downward step as a function of the number of steps in between those two steps. (a) and (b) show the data for steps on the $(11\bar{2}0)$ and $(10\bar{1}0)$ surfaces, respectively.

compound semiconductors, where steps were found to be disassembled[24] and where vacancy migration is initiated by the tip of the STM.[25–27] The changes of the step structure are clearly nonthermal, because if the tip is retracted from the surface no changes occured. Thus, the effect is entirely tip induced. We believe that the mechanisms initiating the transfer of atoms from the surface to the tip are similar to those found on (110) cleavage surfaces of III-V semiconductors.

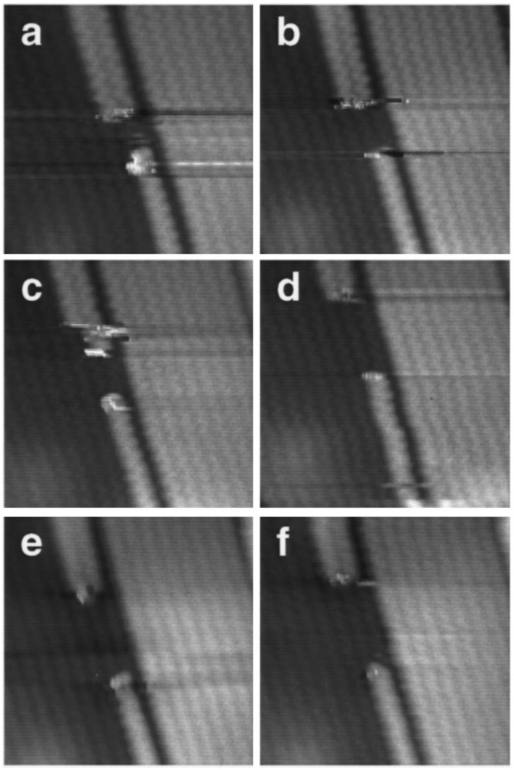

FIG. 12. Series of STM images of a step. The tip modifies the step at the kink sites. The time between the measurement of the first and the last frame is about 3 min. The images were aquired at −2.8 V and 0.2 nA.

IV. DISCUSSION OF THE CLEAVAGE PROCESS

A variety of mechanisms have been proposed for the formation of steps on surfaces. On the one hand, for thermally treated surfaces, the steps frequently arise due to an overall misorientation of the sample surface with respect to low-energy surface orientations. Such steps can be formed in thermal equilibrium at high temperature and are then preserved during a quench to room temperature. On the other hand, steps on cleavage surfaces cannot generally be assumed to be in thermal equilibrium. They occur as a result of a high-energy event in a far-from-equilibrium situation and, therefore, are rather noneqilibrium steps formed by the kinetics of the crack propagation. For example, it has been shown that nonlinear lattice-dynamic instabilities lead to the formation of heavily stepped GaAs(110) surfaces.[28] Such step structures exhibiting triangular-step arrangements have frequently been observed on GaAs(110) surfaces.[29–31] The typical steps on cubic compound semiconductor cleavage surfaces are randomly distributed and all step orientations can be found on one sample.[20] This is one major difference between the steps observed on the cubic and wurtzite compound semiconductor cleavage surfaces. As shown in Fig. 1 the steps on wurtzite cleavage surfaces are all parallel and nearly kink-free.

Another difference between steps on cubic and wurtzite compound semiconductors can be found in the electrical properties of the steps. On cubic compound semiconductor-cleavage surfaces all steps are electrically charged, irrespective of their orientation.[20] On InP(110) surfaces only after heat treatment, one particular step orientation is found to compensate its electrical charge by P evaporation,[20] but this is irrelevant for the cleavage process. On the CdSe surfaces the steps parallel to the [0001] direction are uncharged. From the observed charge of the kinks we conclude that other step orientations would be electrically charged, but they were not formed by cleavage. This points to a particularly large influence of the electrical charge state of the step on the cleavage process. This is not surprising, since the nonpolar planes in compound semiconductors are the preferred cleavage planes because of their electrical properties, which lead to the formation of uncharged surfaces with equal numbers of anions and cations. This view is further corroborated by the fact that cleavage steps on Si(111) surfaces were reported to occur in many orientations.[32] These steps do not exhibit electrical charges.

Finally, the steps observed on the CdSe cleavage surfaces form facets of other nonpolar cleavage surfaces. Steps on cubic compound semiconductors do not form preferred facets. Thus, the particular structure of the facets on CdSe surfaces needs to be considered in the following.

The high-step densities observed on the CdSe surfaces may be due to nonlinear lattice-dynamic instabilities,[28] but this in itself appears to be insufficient to explain the step structure. Therefore, we focus rather on the crack propagation in the wurtzite structure. In the Griffith model of mode I brittle fracture the critical stress σ for a crack of length c to expand spontaneously is given by $\sigma=\{(2\gamma E)/(\pi c)\}^{1/2}$, where Young's modulus E is characteristic of the bond strength and number of bonds of the highly strained material at the crack tip. The energy of the created flanks of the crack is proportional to the surface energy γ. We first discuss the energy of the created surfaces. Compared to all polar surfaces the energy of nonpolar surfaces created by the crack is lower, because no charged surfaces are created, and thus no electrostatic forces have to be overcome during fracture of the crystal. In addition the energy of both nonpolar surfaces is expected to be very close, because the density of atoms on the surface, the number of dangling bonds per atom, and the relaxation mechanism are essentially equal. The cleavage surfaces are both stabilized by an electron transfer from the dangling bond above the cation to that above the anion. The electron transfer is coupled with an outward relaxation of the anion relative to the cation.[3–16] Now we discuss the bond strength. The number of bonds per surface area, nearly equal for most orientations, do not provide any orientational preference. The charge affects, however, the bond strength, such that the bonds between oppositely charged surfaces are stronger, because breaking these bonds require additional electrostatic work compared to nonpolar surfaces. Therefore, the critical stress is largely governed by the electrostatics during cleavage and both the surface energy and the bond strength favor equally a crack propagation in both cleavage planes, but not in polar planes. Similarly, if the steps would be charged, only few steps are to be expected to be created by cleavage. Furthermore, wurtzite-structure crystals have 12 nonpolar cleavage planes separated from each other by 30°. All cleavage planes include the [0001] direction, along which the samples were cleaved. Thus, the geometric relation of the different planes make it quite conceivable that the crack propagates at short intervals in one, two, or three of these planes simultaneously on a microscopic level. This view is supported by the fact that the macroscopic structure of the cleavage surface also exhibited surface areas with orientations of neighboring cleavage planes. Such crack propagation in competing cleavage planes adequately explains the observation of facets at step edges of the neighboring cleavage planes. These facets are also nonpolar cleavage planes. From the discussion it is plausible that the fact that the steps are uncharged favors this type of crack propagation, because the cleavage does not need to overcome any charge-induced forces. The orientation of the steps also supports the crack propagation in competing cleavage planes, because the [0001] direction is the only common intersection line of all the cleavage planes. No other step orientation were found unlike on (110) surfaces of, e.g., InP and GaAs. Any deviation from the [0001] intersection line is equivalent to the formation of a kink. A creation of a kink means a sudden formation of electrical charges. The additional charge can be expected to increase the cleavage energy.

V. SUMMARY

We investigated the atomic structure and the electronic properties of cleavage steps on CdSe $(11\bar{2}0)$ and $(10\bar{1}0)$ surfaces by scanning tunneling microscopy. Steps occur in high concentrations and are always oriented parallel to the [0001] direction on both cleavage surfaces. The steps are electrically uncharged. Kinks are extremely rare and electrically charged. The edges of steps on the $(11\bar{2}0)$ surfaces consist of 1×1 reconstructed $\{10\bar{1}0\}$ facets and steps on $(10\bar{1}0)$ surfaces exhibit 1×1 reconstructed $\{11\bar{2}0\}$ facets. Steps occur preferentially in up and down pairs on both surfaces. The tip can modify steps at kink sites. The step structure is explained by crack propagation in neighboring cleavage planes favored by the creation of uncharged steps.

ACKNOWLEDGMENTS

The authors thank K. H. Graf for technical assistance and the Deutsche Forschungsgemeinschaft for financial support under Grant No. UR 51/2-1.

---

*Author to whom correspondence should be addressed. Electronic address: p.ebert@fz-juelich.de

[1] D. Haneman, Rep. Prog. Phys. **50**, 1045 (1987).

[2] Ph. Ebert, M. Feuerbacher, N. Tamura, M. Wollgarten, and K. Urban, Phys. Rev. Lett. **77**, 3827 (1996).

[3] C. B. Duke, A. Paton, Y. R. Wang, K. Stiles, and A. Kahn, Surf. Sci. **197**, 11 (1988).

[4] A. Kahn, C. B. Duke, and Y. R. Wang, Phys. Rev. B **44**, 5606 (1991).

[5] T. N. Horsky, G. R. Brandes, K. F. Canter, C. B. Duke, A. Paton, D. L. Lessor, A. Kahn, S. F. Horng, K. Stevens, K. Stiles, and A. P. Mills, Jr., Phys. Rev. B **46**, 7011 (1992).

[6] T. N. Horsky, G. R. Brandes, K. F. Canter, C. B. Duke, S. F. Horng, A. Kahn, D. L. Lessor, A. P. Mills, Jr., A. Paton, K. Stevens, and K. Stiles, Phys. Rev. Lett. **62**, 1876 (1989).

[7] C. B. Duke, Chem. Rev. **96**, 1237 (1996).

[8] C. B. Duke, D. L. Lessor, T. N. Horsky, G. R. Brandes, K. F. Canter, P. H. Lippel, A. P. Mills, Jr., A. Paton, and Y. R. Wang, J. Vac. Sci. Technol. A **7**, 2030 (1989).

[9] C. B. Duke and Y. R. Wang, J. Vac. Sci. Technol. A **6**, 692 (1988).

[10] K. O. Magnusson and S. A. Flodström, Phys. Rev. B **38**, 6137 (1988).

[11] J. Pollmann, P. Krüger, M. Rohlfing, S. Sabisch, and D. Vogel, Appl. Surf. Sci. **104/105**, 1 (1996).

[12] P. Schröer, P. Krüger, and J. Pollmann, Phys. Rev. B **49**, 17 092 (1994).

[13] Y. R. Wang, C. B. Duke, K. Stevens, A. Kahn, K. O. Magnusson,

and S. A. Flodström, Surf. Sci. Lett. **206**, L817 (1988).

[14] Y. R. Wang and C. B. Duke, Surf. Sci. **192**, 309 (1987).

[15] C. B. Duke and Y. R. Wang, J. Vac. Sci. Technol. B **6**, 1440 (1988).

[16] Y. R. Wang, C. B. Duke, and C. Mailhiot, Surf. Sci. Lett. **188**, L708 (1987).

[17] J. E. Northrup and J. Neugebauer, Phys. Rev. B **53**, 10 477 (1996).

[18] B. Siemens, C. Domke, Ph. Ebert, and K. Urban, Phys. Rev. B **56**, 12 321 (1997).

[19] Xun Chen, Fang Wu, Zhenyu Zhang, and M. G. Lagally, Phys. Rev. Lett. **73**, 850 (1995).

[20] M. Heinrich, C. Domke, Ph. Ebert, and K. Urban, Phys. Rev. B **53**, 10 894 (1996).

[21] B. Siemens, C. Domke, M. Heinrich, Ph. Ebert, and K. Urban, preceding paper, Phys. Rev. B **59**, 2995 (1999).

[22] J. F. Zheng, X. Liu, N. Newman, E. R. Weber, D. F. Ogletree, and M. Salmeron, Phys. Rev. Lett. **72**, 1490 (1994).

[23] C. Domke, Ph. Ebert, M. Heinrich, and K. Urban, Phys. Rev. B **54**, 10 288 (1996).

[24] Ph. Ebert and K. Urban, Surf. Sci. **287-288**, 891 (1993).

[25] Ph. Ebert, M. G. Lagally, and K. Urban, Phys. Rev. Lett. **70**, 1437 (1993).

[26] G. Lengel, J. Harper, and M. Weimer, Phys. Rev. Lett. **76**, 4725 (1996).

[27] S. Gwo, A. R. Smith, and C. K. Shih, J. Vac. Sci. Technol. A **11**, 1644 (1993).

[28] M. A. Rosentreter, M. Wenderoth, N. H. Theurkauf, A. J. Heinrich, M. A. Schneider, and R. G. Ulbrich, Phys. Rev. B **56**, 10 538 (1997); Europhys. Lett. **38**, 675 (1997).

[29] R. Möller, R. Coenen, B. Koslowski, and M. Rauscher, Surf. Sci. **217**, 289 (1989).

[30] G. Cox, K. H. Graf, D. Szynka, U. Poppe, and K. Urban, Vacuum **41**, 591 (1990).

[31] Y.-N. Yang, B. M. Trafas, R. L. Siefert, and J. H. Weaver, Phys. Rev. B **44**, 3218 (1991).

[32] R. M. Feenstra and J. A. Stroscio, Phys. Rev. Lett. **59**, 2173 (1987).